Electronic Supplementary Material (ESI) for Catalysis Science & Technology.

Supporting Information for Publication

DNA Enthralled Less Resistive Palladium Nano-Spheres for Effective Hydrogen Evolution Reaction

Sangeetha Kumaravel,[†‡] Karthik Kumaran Saravanan,[†] Bariki Eunice Evangeline,[†]
Vennala Niharika,[†] Rishivandhiga Jayakumar[†] and Subrata Kundu[†‡*]

[†]*Electrochemical Process Engineering (EPE) Division, CSIR-Central Electrochemical Research Institute (CECRI), Karaikudi-630003, Tamil Nadu, India.*

[‡] *Academy of Scientific and Innovative Research (AcSIR), Ghaziabad-201002, India.*

*To whom correspondence should be addressed, *E-mail: skundu@cecri.res.in and kundu.subrata@gmail.com*, Tel: +91 4565-241487.

This file contains pages from S1 to S27, where the detailed, reagents and instruments used in the study, figures and Tables corresponding to Pd/DNA are provided.

Number of Pages: 27

Number of Figures: 19

Number of Tables: 02

Reagents and Instruments

The precursor, Palladium (II) nitrate ($Pd(NO_3)_2 \cdot xH_2O$) were purchased from Aldrich and the reducing agent Sodium borohydride ($NaBH_4$) were received from Sigma-Aldrich. The biomolecule Double stranded Deoxyribonucleic acid (dsDNA) was received from Sigma-Aldrich (99%) which is having a base pair of 50 k. Saturated calomel electrode (SCE) (reference electrodes) and the CC (counter electrode) were purchased from Alfa- Aesar. Aut-M204 was used for the entire electrochemical HER study. Distilled water was used for the synthesis of different concentrated Pd/DNA catalyst. The DNA stabilized Pd/DNA electro catalyst was characterized using the following techniques such as UV-Vis, FT-IR, HR-TEM, EDS, HAADF, XRD, and XPS analysis. The UV-Visible (UV-Vis) absorption spectrum was recorded in a Unico (model 4802) UV-Vis-NIR spectrophotometer equipped with a 1 cm quartz cuvette holder for liquid samples. The Fourier Transform Infrared (FT-IR) spectroscopy analysis carried in the model Nexus 670 (FTIR), Centaurms 10X (Microscope) with the spectral range 4,000 to 400 cm^{-1} with a MCT-B detector. The X-ray diffraction (XRD) analysis was carried out using a PAN analytical Advanced Bragg-Brentano X-ray powder diffractometer (XRD) with Cu K_α radiation ($\lambda = 0.154178$ nm) with a scanning rate of 5° min^{-1} in the 2θ range 10-80°. The morphological studies and the HAADF colour mapping of both the electrocatalyst was carried in HR-TEM, (TecnaiTM G2TF20) working at an accelerating voltage of 200 kV. The Energy Dispersive X-ray Spectroscopy (EDS) analysis was done with the HR-TEM with a separate EDS detector (INCA) connected to that instrument. The X-ray photoelectron spectroscopic (XPS) analysis was done to check the state of elements present in the outermost part of materials and analysed by using Theta Probe AR-XPS System, Thermo Fisher Scientific (U.K). The X-ray fluorescence (XRF) analysis was carried out using XGT-5200 X-ray analytical microscope with X-ray tube 50 kV max, 1 mA, with Rh target (0-40 keV). Electrochemical analyzer AUT-M204 was used for the entire HER and related studies.

Synthesis of Palladium NPs for electrochemical studies

The pure palladium NPs were prepared for the comparison studies with Pd/DNA. Here, 0.1 M $PdCl_2$ was dissolved in 10 mL of DI water. After that 0.1 M $NaBH_4$ was added with the above solution, here the addition of reducing agent reduces the Pd^{2+} to Pd^0 and got settled down. Then the supernatant liquid was discarded, the Pd NPs were washed thoroughly and kept at drying for overnight. This Pd NPs were used for the comparative studies with the loading of 0.205 mg cm^{-2} over carbon cloth.

Preparation of DNA stock solution

The DNA powder received was dispersed with the 100 mL of DI water. The DNA was taken as 0.12 M in aqueous solution and kept at stirring for overnight to achieve the clear solution. This dispersed DNA solution was utilized for the preparation Pd NSs.

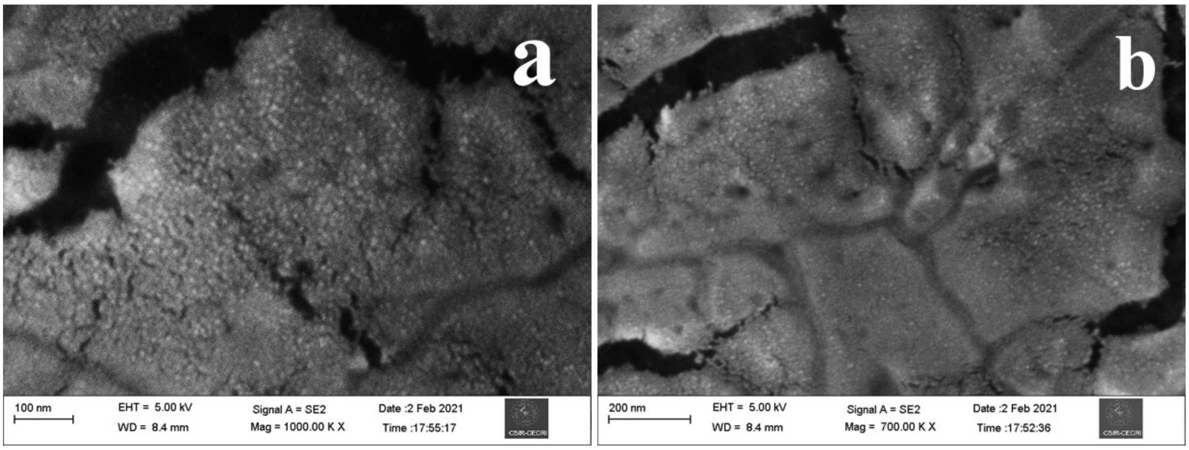

Figure S1. (a and b) The high and low magnified FE-SEM images of Pd/DNA (0.06) NSs.

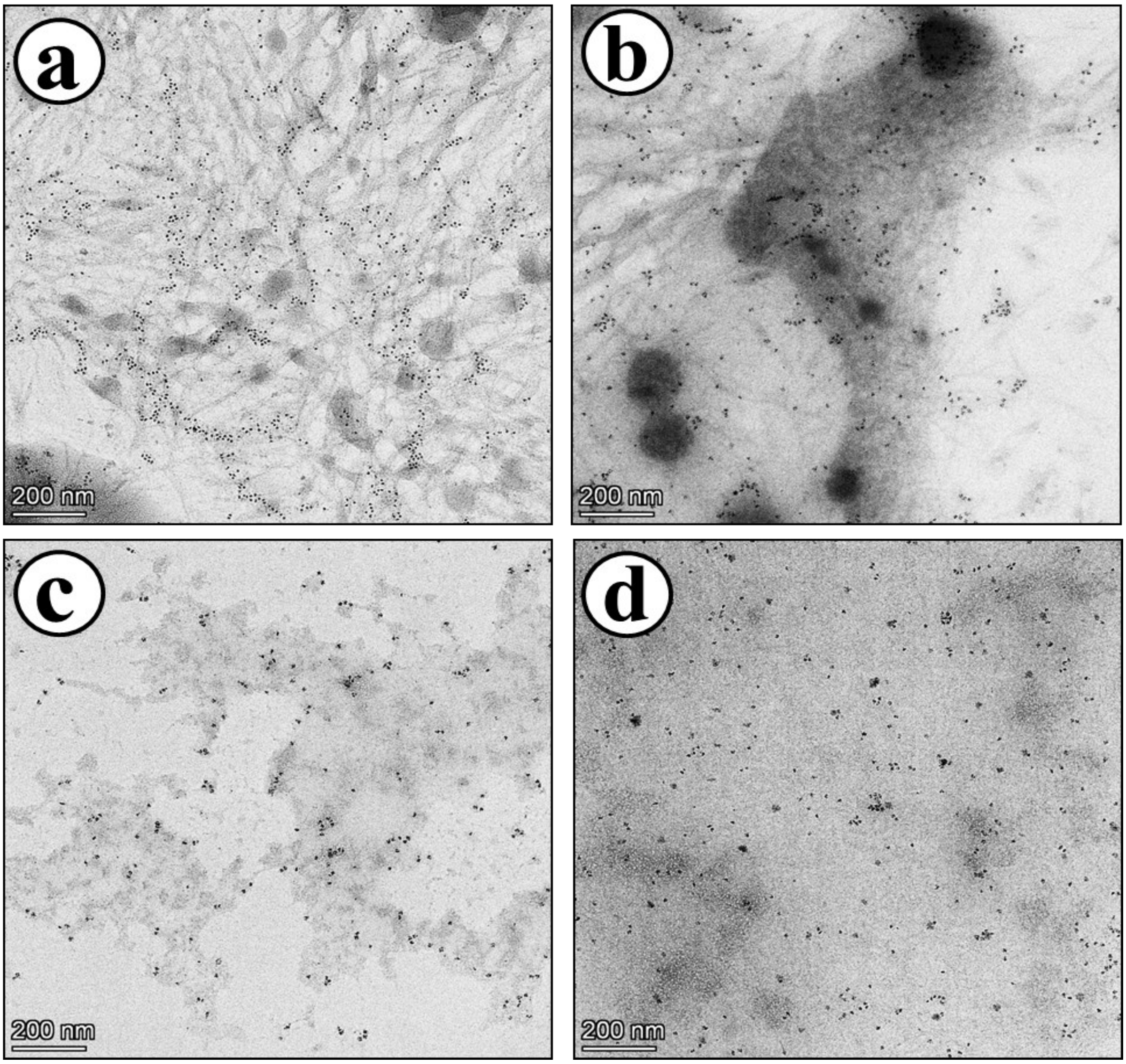

Figure S2. (a-d) The low and high magnified HR-TEM images of sets of Pd NSs prepared using varying DNA concentrations such as Pd/DNA (0.048) (a), Pd/DNA (0.072) (b), Pd/DNA (0.096) (c) and Pd/DNA (0.1) (d), respectively.

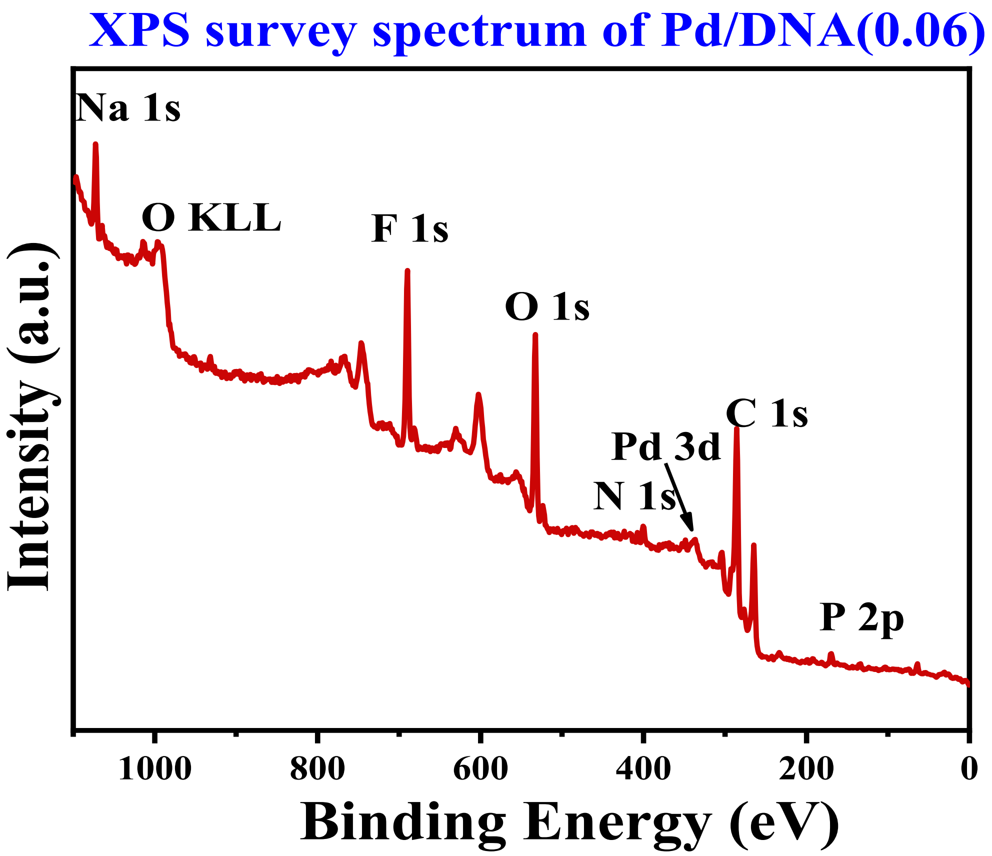

Figure S3. X-ray photoelectron (XPS) survey spectrum of Pd/DNA (0.06).

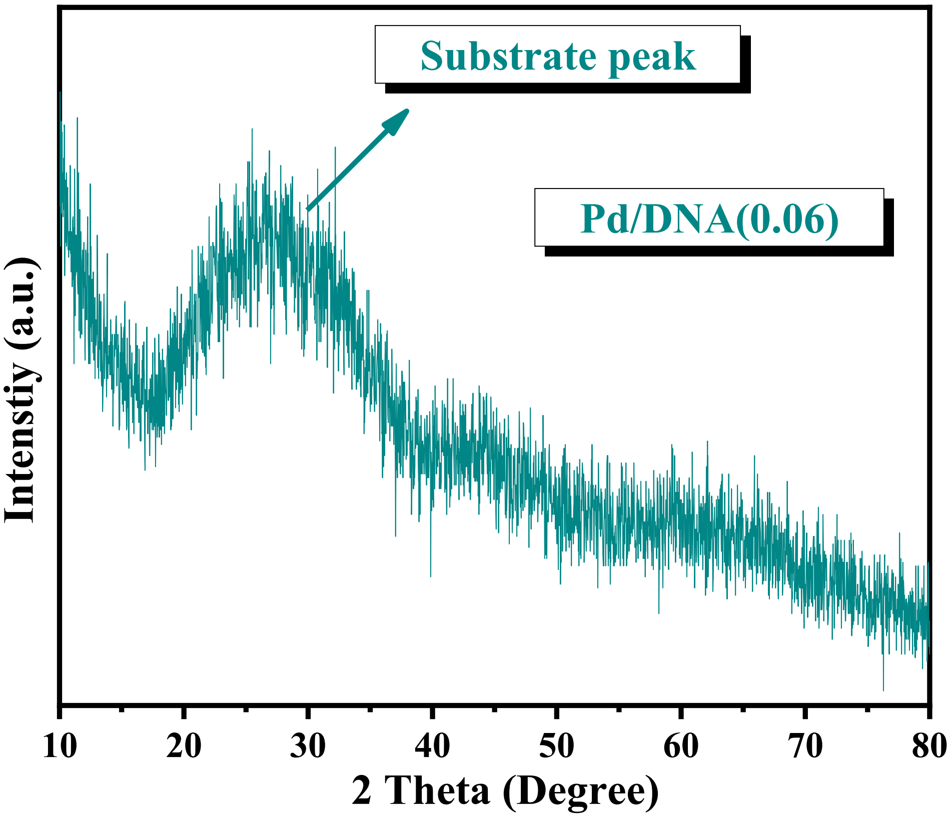

Figure S4. XRD pattern for Pd/DNA NSs.

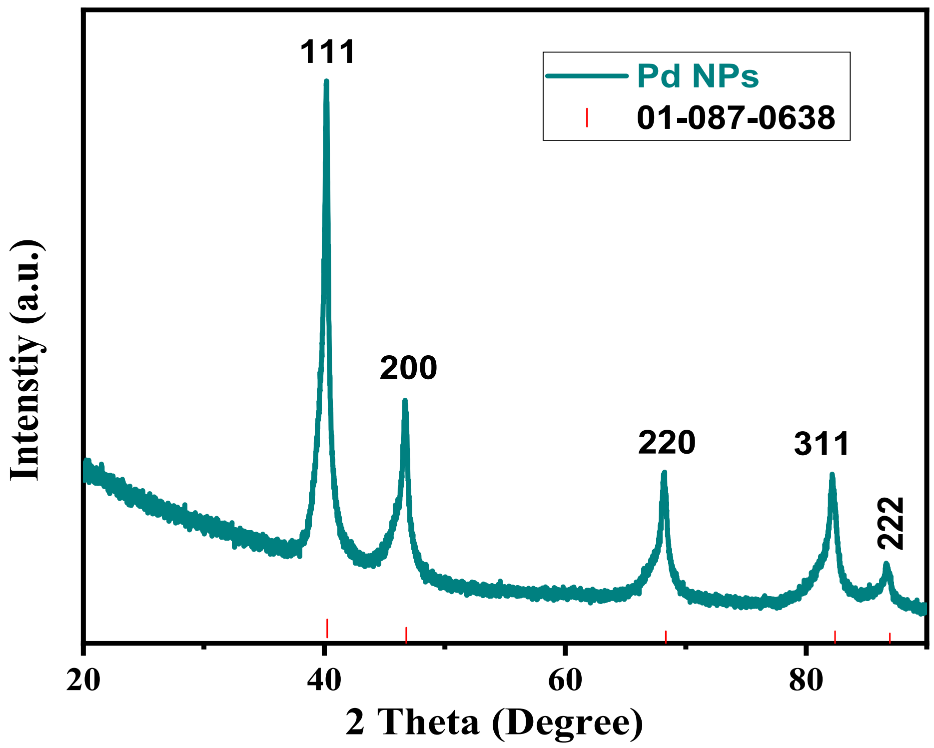

Figure S5. XRD pattern of the bare Pd NPs.

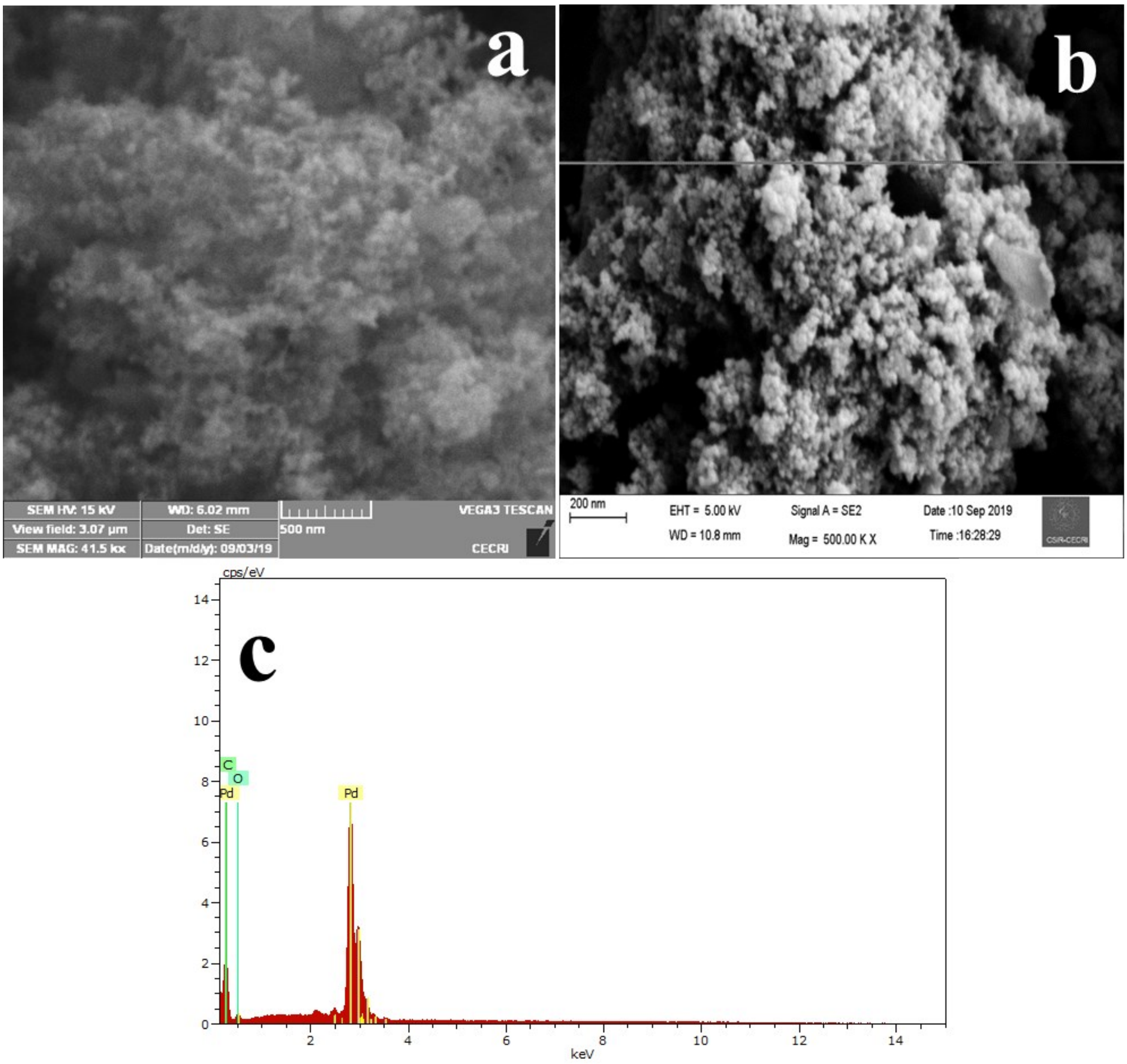

Figure S6. (a and b) are the SEM and FE-SEM images of bare Pd NPs and (c) is the EDS analysis of the bare Pd NPs.

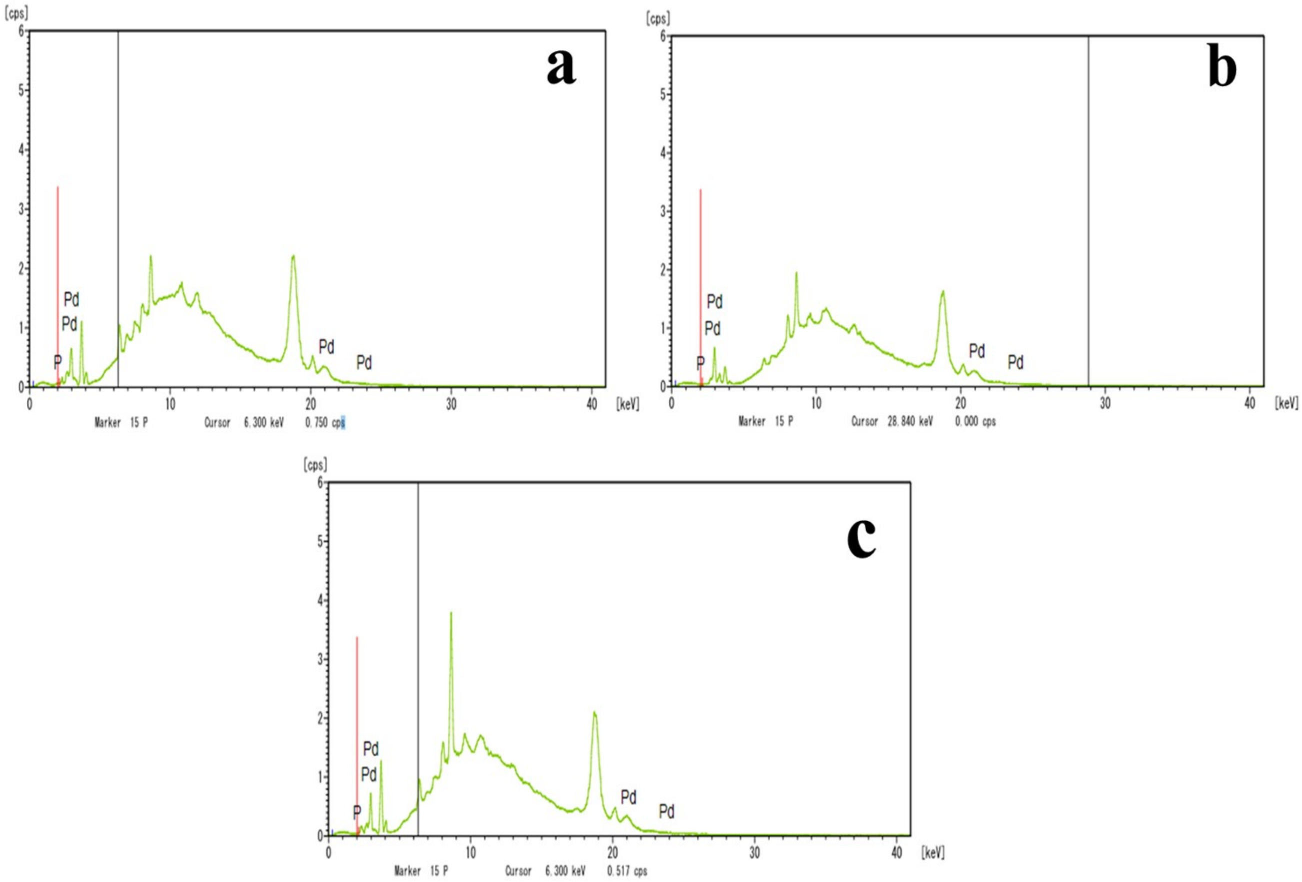

Figure S7. XRF analysis of varying DNA concentrated Pd NSs such as (a) Pd/DNA (0.048); (b) Pd/DNA (0.06) and (c) Pd/DNA (0.072) respectively.

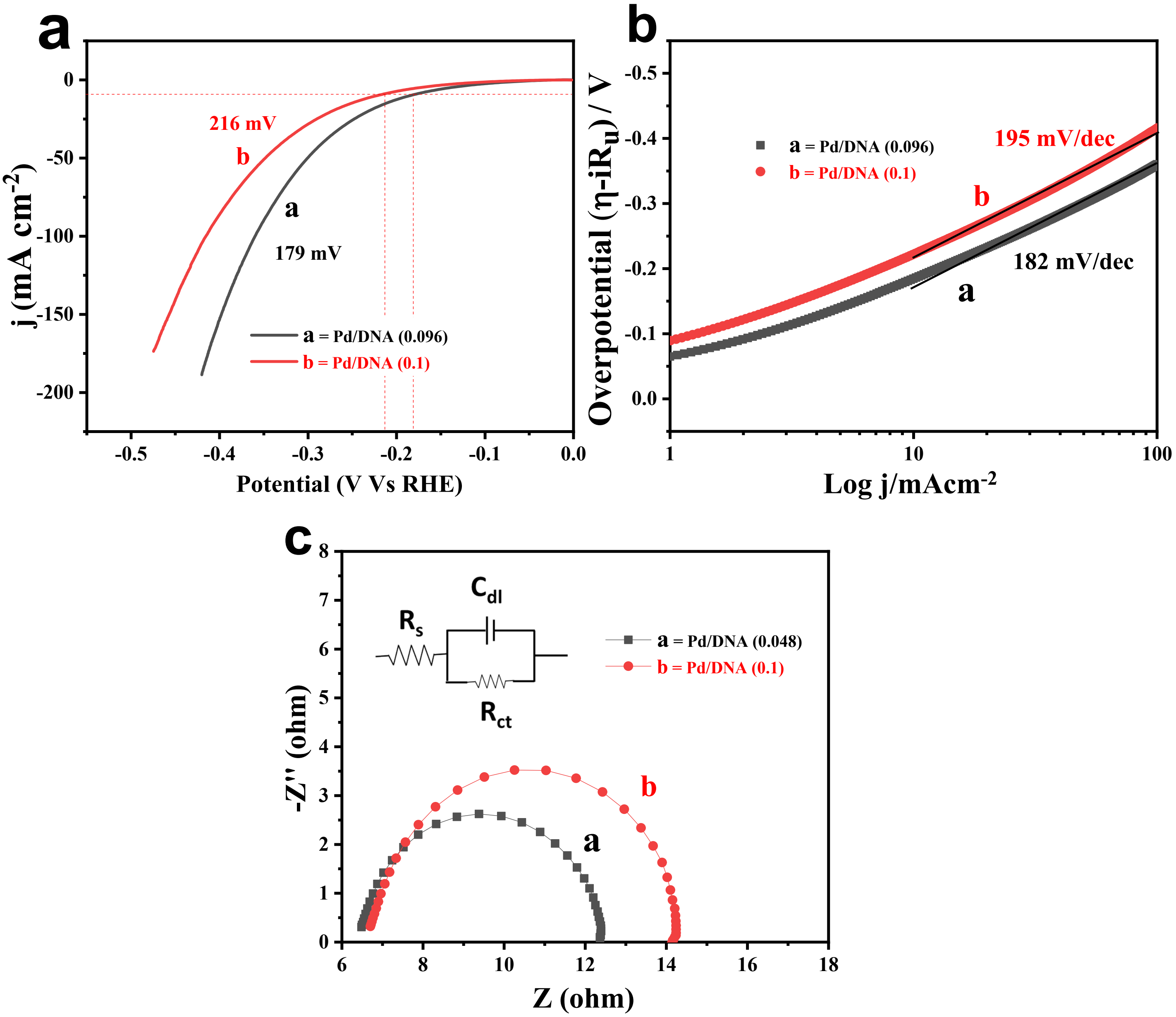

Figure S8. Electrochemical HER studies of Pd/DNA with increased DNA conc. (a) the LSV analysis of Pd/DNA (0.096 and 0.1); (b and c) is the corresponding Tafel slope and EIS analysis of the same.

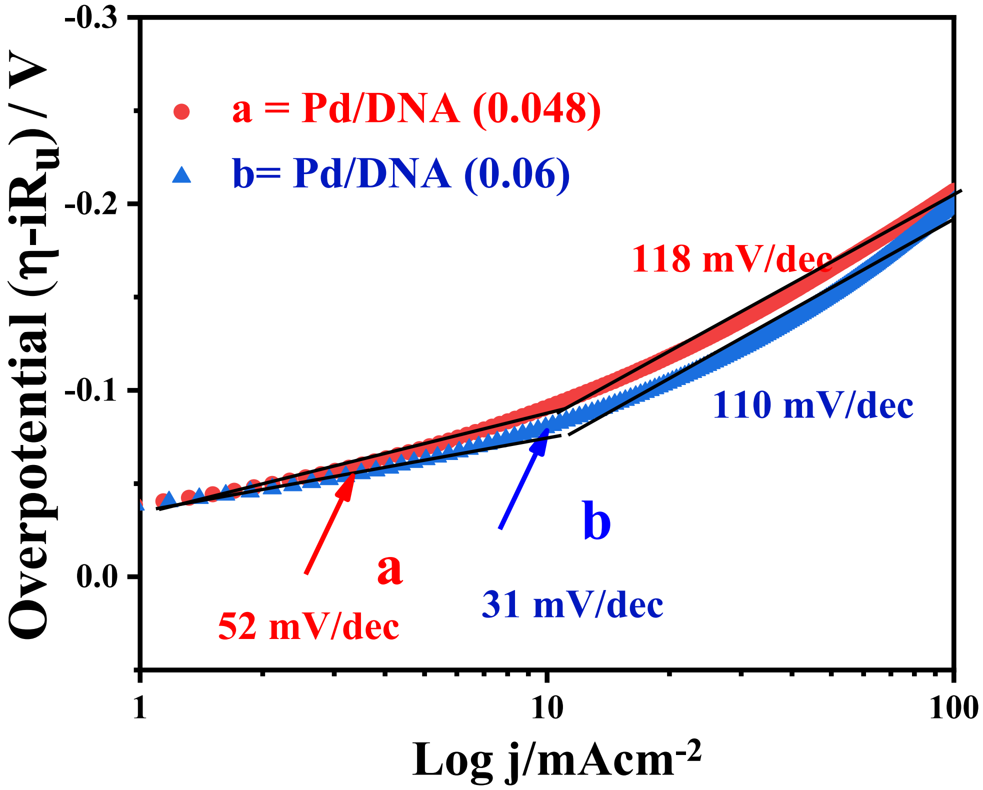

Figure S9. Tafel analysis of Pd/DNA (0.06) with both low and high overpotential region.

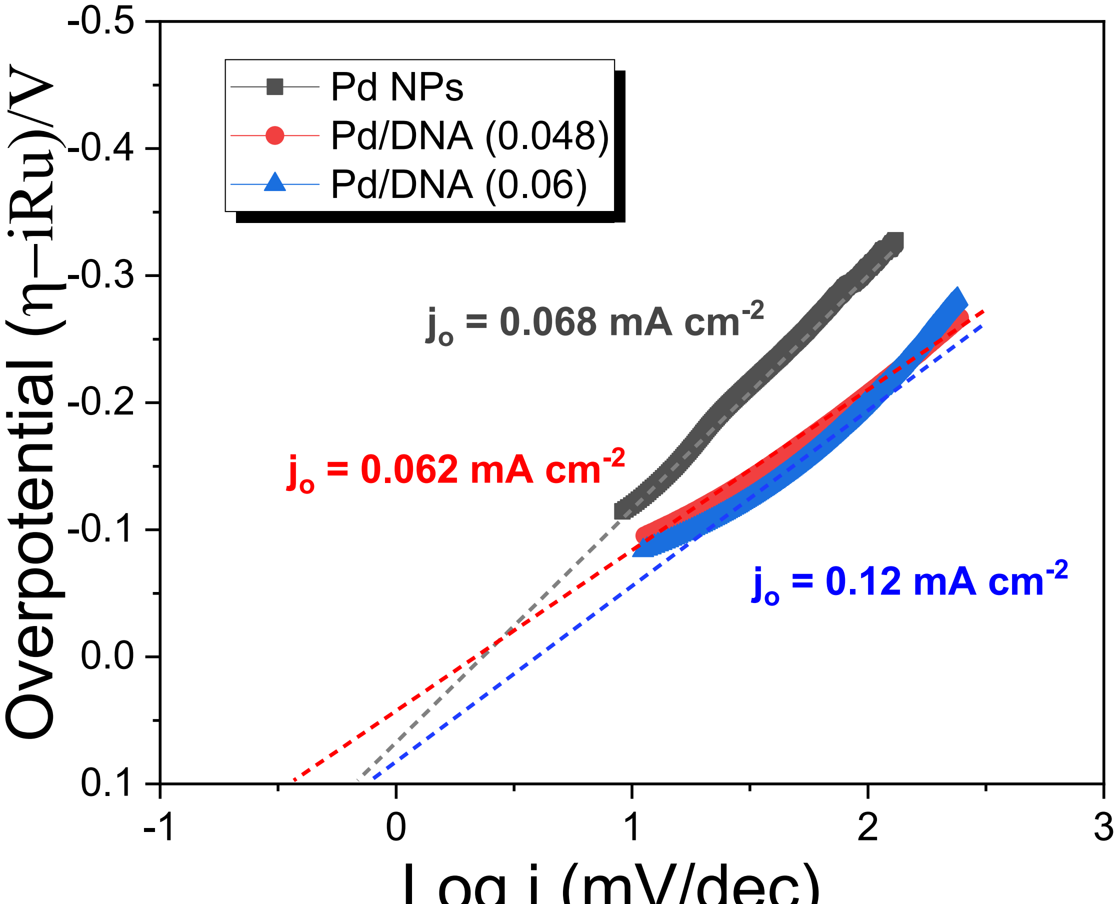

Figure S10. Exchange current densities of Pd/DNA electrocatalysts calculated from the Tafel slope.

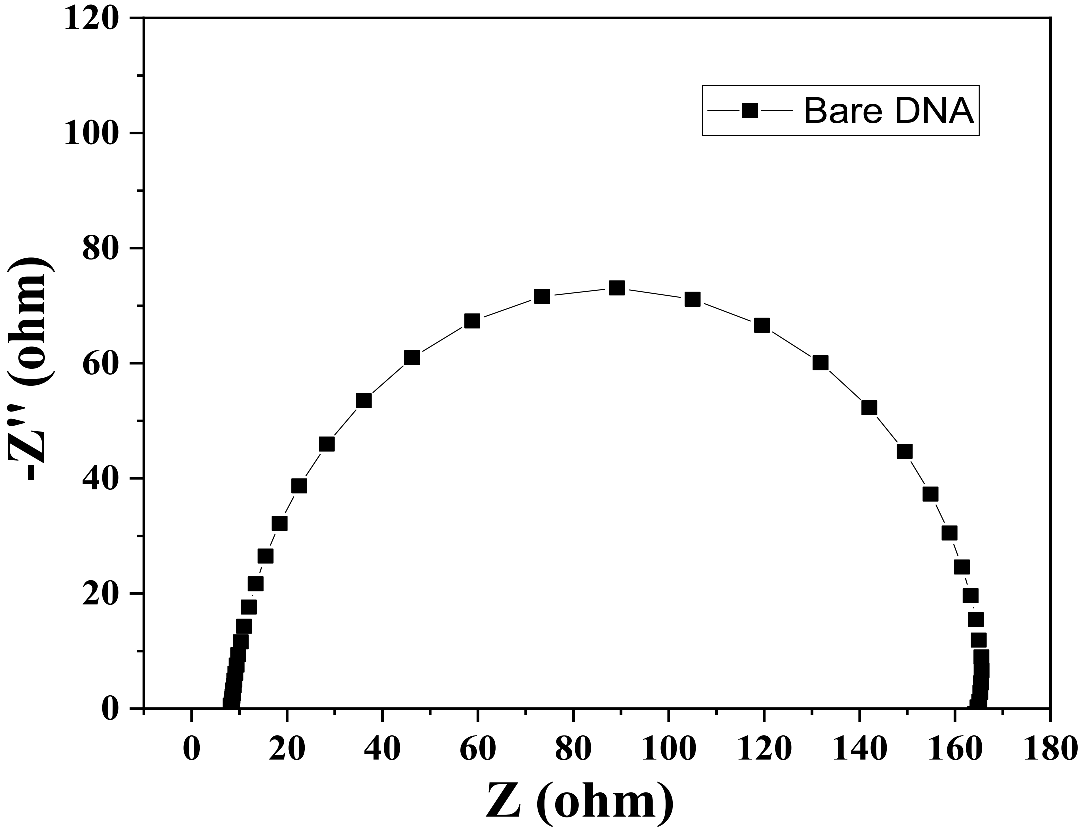

Figure S11. EIS spectra of bare DNA.

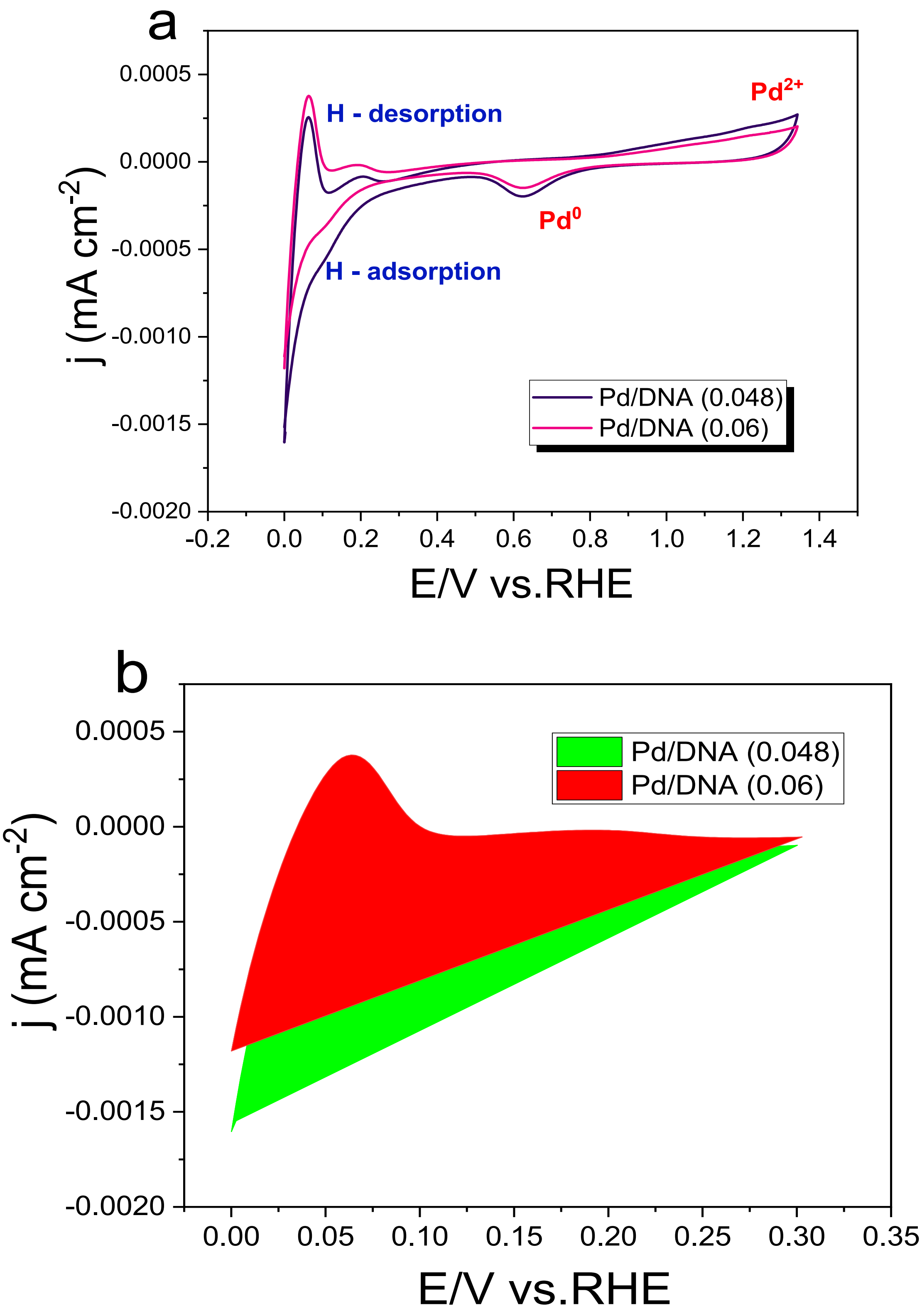

Figure S12. (a) H-desorption peak from the near anodic region in HER in acid and (b) corresponding area chosen for the charge associated with it for ECSA.

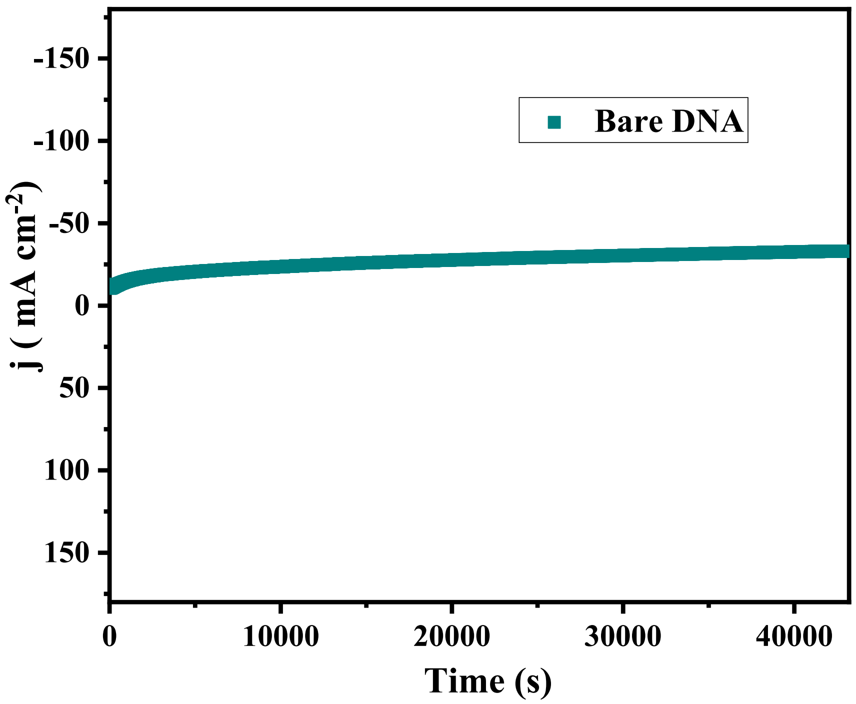

Figure S13. Chronoamperometric study of bare DNA for 12 h.

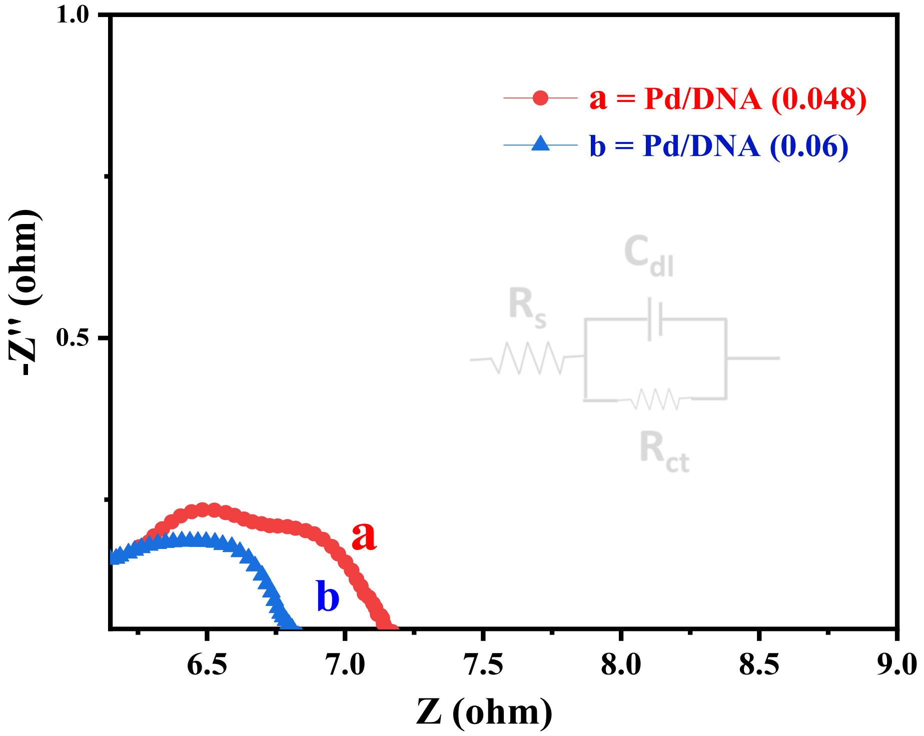

Figure S14. Post EIS analysis of the electrocatalyst Pd/DNA (0.048 and 0.06) with the equivalent circuit.

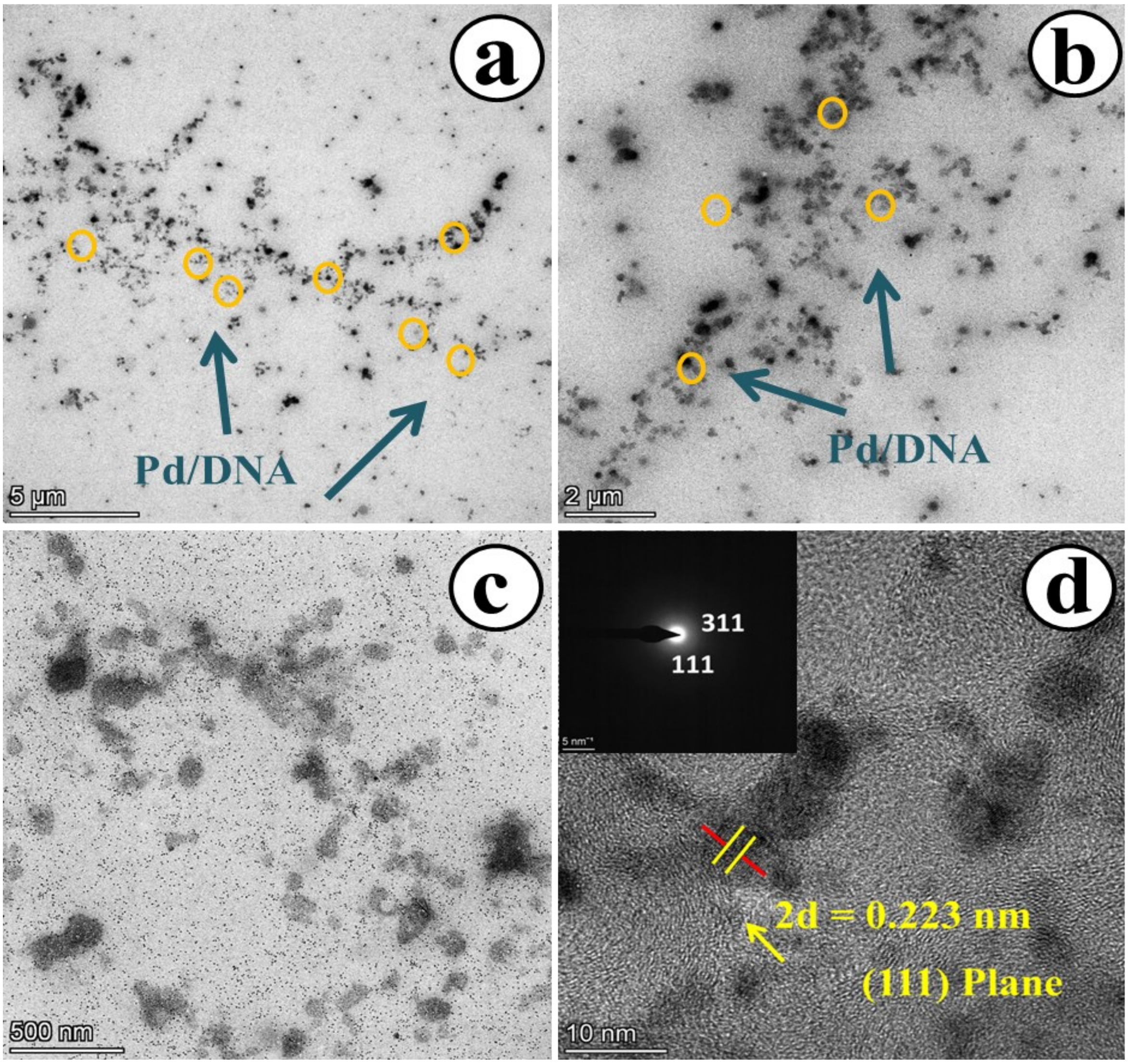

Figure S15. (a-c) are the post morphological analysis of Pd NPs over DNA (0.06) and (d) is the lattice fringes for same. Inset of (d) is the SAED pattern of Pd/DNA (0.06).

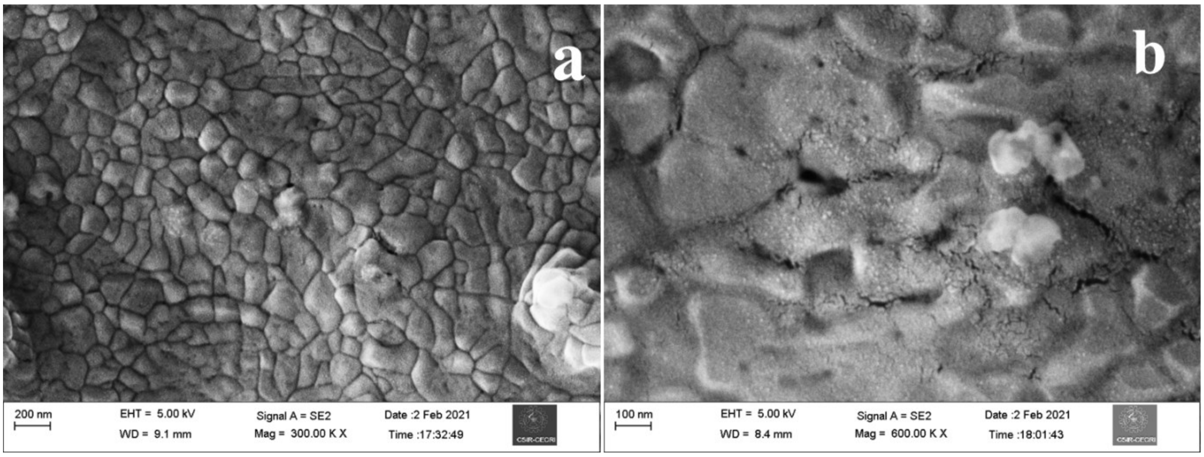

Figure S16. The high and low magnified (a and b) post FE-SEM images of Pd/DNA (0.06) NSs.

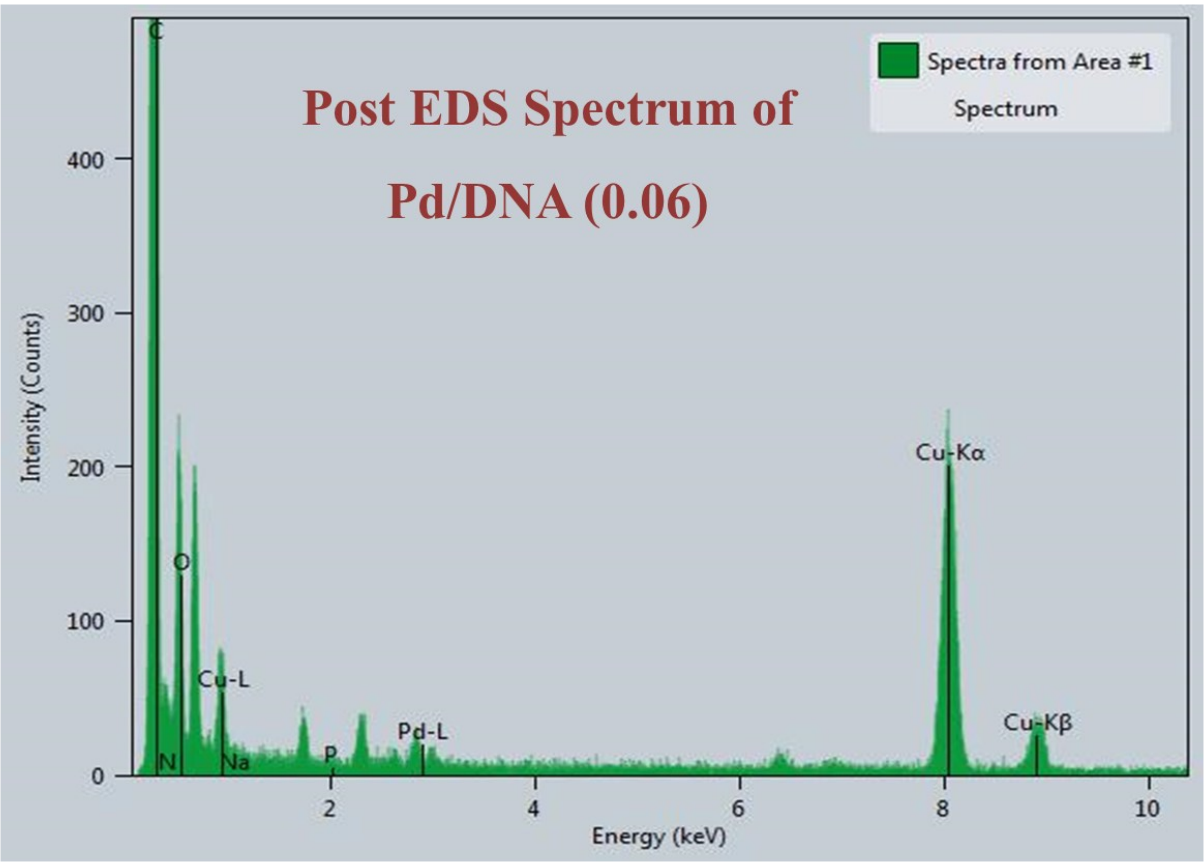

Figure S17. Post Energy dispersive X-ray spectrum of Pd/DNA (0.06) shows the elemental presence of Pd O, C, N and P.

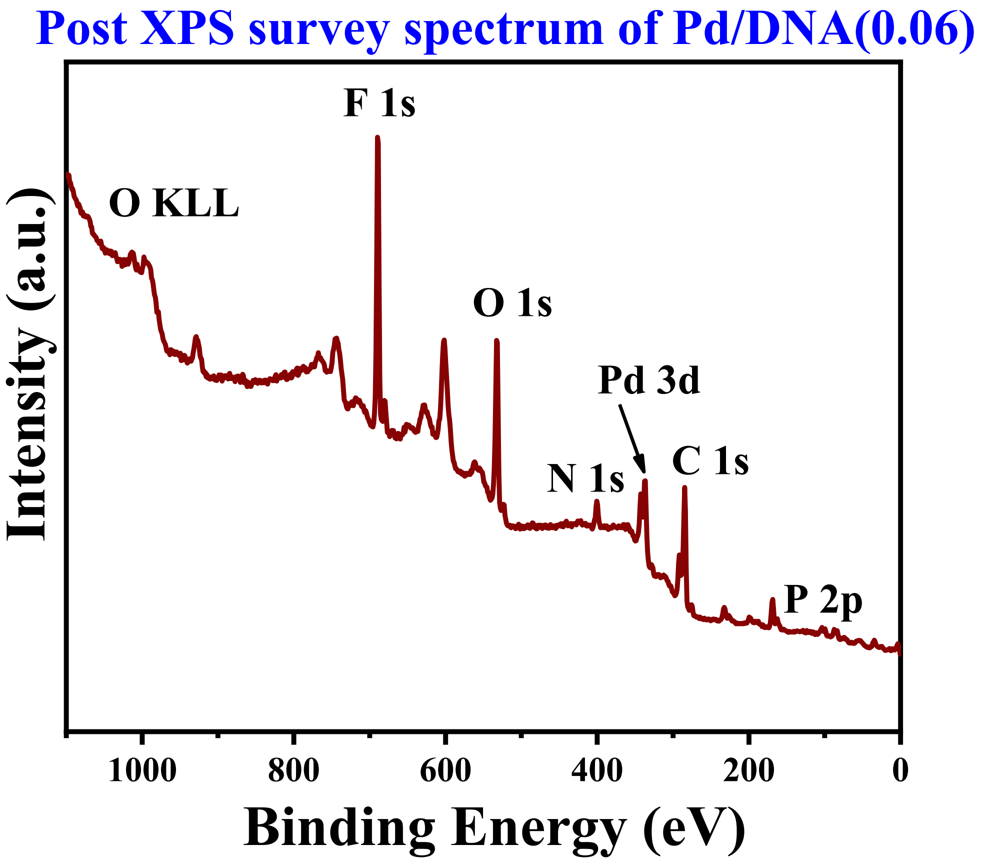

Figure S18. Post X-ray photoelectron (XPS) survey spectrum of Pd/DNA (0.06).

Figure S19. Photo image of stable aqueous stabilized Pd/DNA (0.06).

Table S1. Optimization information of stable Pd NSs over DNA.

S. No	Volume of 10^{-2} M $Pd(NO_3)_2 \cdot xH_2O$ Solution (mL)	Volume of DNA(mL) (0.12 M)	Volume of (0.1 M) $NaBH_4$ solution (mL)	Conc. of DNA (M)	Observation	Solution state
1.	1	3	1	0.036	Brown	Settled
2.	1	4	1	0.048	Brown	Stable
3.	1	5	1	0.06	Brown	Stable
4.	1	6	1	0.072	Brown	Stable
5.	1	7	1	0.084	Brown	Stable
6.	2	8	1	0.096	Brown	Stable
7.	3	10	1	0.1	Brown	Stable

Table S2. Comparison of HER performance of Pd/DNA (0.06) catalyst with other Pd based catalyst in terms of current density, loading, overpotential and Tafel slope.[1,2,11–20,3–10]

S. No.	Catalyst	Loading mg cm^2	Current density mA cm^{-2}	Overpotential (mV)	Tafel slope (mV dec^{-1})	References
1	PdTe	-	10	97	90	*Nanoscale,* 2015, **7**, 18441–18445.
2	Pd_7Se_4	-	10	162	56	*Chem. Commun*., 2016, **52**, 206–209.
3	$PdBi_2$	0.28	10	78	63	*J. Mater. Chem. A,* 2017**, 5**, 15950–15960.
4	Pd_2Si	1	10	243	-	*Inorg. Chem.,* 2015, **54,** 707–709.
5	Pd/C	-	10	80	81	*Ionics* **26,** 1347–1356 (2020).
6	Pd nanocubes	-	10	51	62	*J. Power Sources,* 2016, **302**, 343–351.
7	rGO-PdPS	0.003	10	100	46	*Chem. Commun.,* 2014, **50,** 7359–7362.
8	Pd/$Ti_3C_2T_x$–CNT	0.4	10	158	50	*j.ceramint.*2020. 11.**151**, (2020).

9	Pd NP on graphitic carbon nitride	0.043	10	55	35	*ACS Catal.,* 2016**, 6,** 1929–1941.
10	Pd NPs supported on Vulcan	0.7	10	20	-	*J. Power Sources,* 2008, **177**, 281–285.
11	Pd NPs on Vulcan	0.02	-	60	148	*J. Electrochem. Soc.,* 2016, **163**, F499–F506.
12	rGO-$Fe_{48}Pd_{52}$	-	10	250	370	*J. Hydrogen Energy,* 2017, **42**, 3916–3925.
13	f-MWCNTs@Pd/TiO_2	0.16	-	<100	130	*Nat. Commun.,* 2016, **7**, 13549.
14	AgPd alloys	-	-	270	156	*Fuel,* 2014, **118,** 156–162.
15	Pt@Pd	0.281	10	56	39	*ACS Sustainable Chem. Eng.,* 2017, **5**, 8675–8683.
16	PdCo alloy	0.285	10	80	31	*ACS Appl. Mater. Interfaces,* 2016, **8**, 13378–13383.
17	$(Ni/Pd)_{17}Se_{15}$	-	10	197	91.5	*ACS Appl. Energy Mater.* 2020, **4**, 4051–

						4056
18	Ni@Pd	0.14	10	54	54	*J. Mater. Chem. A,* 2015, **3,** 11261–11268.
19	Pd$_x$Cu$_{100-x}$/C	-	10	102	48	*Electrochim. Acta,* 2017, **246**, 572–579.
20	PdNiMo film	-	10	110	227	*Electrochim. Acta,* 2015, 174, 1041–1049.
21	**Pd/DNA (0.06)**	**0.01**	**10**	**79**	**31**	**This work**

References

1 L. Jiao, F. Li, X. Li, R. Ren, J. Li, X. Zhou, J. Jin and R. Li, *Nanoscale*, 2015, **7**, 18441–18445.

2 S. Kukunuri, P. M. Austeria and S. Sampath, *Chem. Commun.*, 2015, **52**, 206–209.

3 S. Sarkar, U. Subbarao and S. C. Peter, *J. Mater. Chem. A*, 2017, **30**, 15950–15960.

4 J. M. Mcenaney and R. E. Schaak, *Inorg. Chem.*, 2014, 707–709.

5 Y. Qu, S. Wen, J. Chen, H. Shen, W. Yu, D. Wei, J. Yu, Y. Kwon and Y. Zhao, *Ionics*, 2019, **26**, 1347–1356.

6 Y. Sun and Y. Xia, *Science*, 2002, **298**, 2176–2180.

7 S. Sarkar and S. Sampath, *Chem. Commun.*, 2014, **50**, 7359–7362.

8 P. Zhang, T. Xiao, Z. Chang, Z. Fang, Z. Zhu and C. Author, *Energy Technol.*, 2020, **8**, 2000306.

9 T. Bhowmik, M. K. Kundu and S. Barman, *ACS Catal.*, 2016, **3**, 1929–1941.

10 S. A. Grigoriev, P. Millet and V. N. Fateev, *J. Power Sources*, 2008, **177**, 281–285.

11 J. Zheng, J. E. Soc, J. Zheng, S. Zhou, S. Gu, B. Xu and Y. Yan, *J. Electrochem. Soc.*, 2016, **163**, F499.

12 D. S. P. Cardoso, M. Sevim, J. A. S. B. Cardoso, L. Amaral, T. Sener, C. A. C. Sequeira and D. M. F. Santos, *Int. J. Hydrogen Energy*, 2016, **42**, 3916–3925.

13 G. Valenti, A. Boni, M. Melchionna, M. Cargnello, L. Nasi, G. Bertoni, R. J. Gorte, M. Marcaccio, S. Rapino, M. Bonchio, P. Fornasiero, M. Prato and F. Paolucci, *Nat. Commun.*, 2016, **7**, 1–8.

14 A. Safavi, S. Habib and H. Kazemi, *Fuel*, 2014, **118**, 156–162.

15 X. Lin, A. Wang, K. Fang, J. Yuan and J. Feng, *ACS Sustain. Chem. Eng.*, 2017, **5**, 8675−8683.

16 J. Chen, G. Xia, P. Jiang, Y. Yang, R. Li, R. Shi, J. Su and Q. Chen, *ACS Appl. Mater. Interfaces*, 2016, **7**, 1–8.

17 S. C. Sarma, S. M. Kaja, K. A. A. Mary and S. C. Peter, *ACS Appl. Energy Mater.*, 2020, **3**, 4051−4056.

18 J. Li, P. Zhou, F. Li, R. Ren, Y. Liu, J. Niu, J. Ma, X. Zhang, M. Tian and J. Ma, *J. Mater. Chem. A*, 2015, **3**, 11261–11268.

19 X. Zhang, D. Wu and D. Cheng, *Electrochim. Acta*, 2017, **246**, 572–579.

20 J. Tang, X. Zhao, Y. Zuo, P. Ju and Y. Tang, *Electrochim. Acta*, 2015, **174**, 1041–1049.